PCCP
Physical Chemistry Chemical Physics

Accepted Manuscript

This article can be cited before page numbers have been issued, to do this please use: G. Horwitz, E. J. Calvo, L. P. P. Méndez De Leo and E. de la Llave, *Phys. Chem. Chem. Phys.*, 2020, DOI: 10.1039/D0CP02568B.

View Article Online
DOI: 10.1039/D0CP02568B

Electrochemical Stability of Glyme-based Electrolytes for Li-O_2 Batteries Studied by In Situ Infrared Spectroscopy

Gabriela Horwitz[a], Ernesto J. Calvo[b], Lucila P. Méndez De Leo[b,*], Ezequiel de la Llave[b,*]

[a]Departamento de Física de la Materia Condensada and Instituto de Nanociencias y Nanotecnología (INN-CONICET), Comisión Nacional de Energía Atómica, Avda. General Paz 1499 (1650), San Martín, Buenos Aires, Argentina.

[b]Departamento de Química Inorgánica, Analítica y Química Física, INQUIMAE-CONICET, Facultad Ciencias Exactas y Naturales, Universidad de Buenos Aires, Ciudad Universidad, Pabellón II, Buenos Aires C1428EHA, Argentina.

KEYWORDS: Lithium, oxygen, battery, glyme, FTIR, SNIFTIRS

*Corresponding authors.

e-mail address: edelallave@qi.fcen.uba.ar. (E. de la Llave).

e-mail address: lucilamdl@qi.fcen.uba.ar (L.P. Méndez De Leo).

View Article Online
DOI: 10.1039/D0CP02568B

ABSTRACT

In situ subtractively normalized Fourier transform infrared spectroscopy (SNIFTIRS) experiments were performed simultaneously with electrochemical experiments relevant to Li-air battery operation on gold electrodes in two glyme-based electrolytes: diglyme (DG) and tetraglyme (TEGDME), tested under different operational conditions. Results show that TEGDME is intrinsically unstable and decomposes at potentials between 3.6 - 3.9 V vs Li^+/Li even in the absence of oxygen and lithium ions, while DG shows a better stability, and only decomposes at 4.0 V vs Li^+/Li in presence of oxygen. The addition of water to the DG based electrolyte exacerbates its decomposition, probably due to the promotion of singlet oxygen formation.

1. INTRODUCTION

The increasing global energy consumption along with the increasing need for new and better energy storage devices have driven the attention of the scientific battery community to high energy density systems such as Li-air batteries (LABs).[1] It is believed that LABs could replace the traditionally used fossil fuels in transportation,[2,3] as they have much higher theoretical energy density than the current Li-ion technologies.[4–6]

However, there are still many challenges to overcome before using this system as a practical energy storage device. One of the main drawbacks is the lack of a suitable and stable electrolyte.[7] Carbonate-based electrolytes, of widespread use in lithium-ion technology, are highly unstable in LABs, decomposing to form lithium carbonate during discharge and evolving CO_2 during charge.[8–10] Bruce and co-workers showed that electrolytes based on ethers,[11] amides[12] and sulfones[13] were found to be unstable on carbon cathodes in LAB configuration. McCloskey et al. analyzed the first galvanostatic charge/discharge cycle of different electrolytes showing that none

View Article Online
DOI: 10.1039/D0CP02568B

of the tested organic electrolytes have a coulombic efficiency greater than ninety percent.[14] Also, many reports have indicated that dimethyl sulfoxide undergoes decomposition during the cycling of the LAB, in the same line as the previously mentioned organic electrolytes.[15–17] In the last years, several reports showed glyme-based cells (mono-, di-, tri- and tetra-glyme: $CH_3{-}O{-}(CH_2{-}CH_2{-}O)_n{-}CH_3$, with n = 1−4) with promising electrochemical performance,[18–20] though there is no general consensus regarding their stability in the conditions of a working battery. Chamaani et al.[21] used ex-situ Raman spectroscopy for studying a LAB containing bis(trifluoromethane) sulfonimide lithium salt (LiTFSI) in tetraglyme (TEGDME), and a cathode of carbon nanotubes deposited on carbon cloth. They concluded that the Li_2CO_3 deposited on the cathode after failure discharge cycles is due to the decomposition of the tetraglyme inside the porous cathode, and that the level of degradation decreases when salt concentration increases. A few years later, Scrosati *et. al.*[19] used $LiCF_3SO_3$ in TEGDME with Super P carbon black and they found no capacity fading after 100 cycles at high specific discharge and charge rate. Gasteiger and co-workers[22] determined via infrared and UV-Vis spectroscopy that all glymes are sufficiently stable against the attack of superoxide anion once they are purified; on the contrary, Aurbach and co-workers[20] showed that proper glyme selection is critical for electrolyte stability on Li-O_2 cells: they tested cell cyclability of LiTFSI in mono-, di-, tri- and tetra-glyme, and found that diglyme is the most stable of the family, without significant capacity fading for more than 50 cycles. It has been proposed that longer glymes are more susceptible to superoxide attack due to the formation of weaker complexes with the lithium cation[20–23] although others have found that monoglyme is more strongly degraded compared to tetraglyme.[24] The reason for all these discrepancies is not certainly known. The work of Wandt et al.[25] followed by Freunberger et al.[26] set a milestone on the understanding of the degradation of electrolytes and cathode materials. The role of the superoxide anion formed during discharge as the main responsible for parasitic reactions was replaced with

View Article Online
DOI: 10.1039/D0CP02568B

the formation of $^1O_2$ – during discharge and charge – which allowed to explain the fact that side reactions are stronger during charge.

The effect of water impurities on the electrochemical performance is another issue in question. It is generally known,[1] that the addition of a certain amount of water to a non-aqueous electrolyte promotes the formation of toroidal shaped Li_2O_2 deposits during the discharge, enabling higher discharge capacity. Despite several attempts made to take advantage of this phenomenon,[27–29] including the use of a redox mediator, the reversibility and mechanism of those complex chemical systems are not agreed upon.

In this work, in order to have some insight into the electrochemical stability of glyme-based electrolytes, we performed in situ infrared spectroscopy experiments along with an electrochemical characterization of two glymes: diglyme (DG) and tetraglyme (TEGDME). We explored what effect on the stability of the electrolyte has the presence or absence of lithium ions, water content and dissolved oxygen. The effect of the nature of the counterions, $CF_3SO_3^-$ (triflate, Tf^-) and $TFSI^-$ was also examined.

2. EXPERIMENTAL

2.1 Materials

Anhydrous bis(2-methoxy-ethyl)ether (diglyme, DG, Sigma-Aldrich, 99.5% pure) and triethylene glycol dimethyl ether (TEGDME, Sigma-Aldrich, 99.0% pure), lithium trifluoro-methanesulfonate (Li triflate, Sigma-Aldrich, 99.99%), tetrabuthylammonium trifluoromethane-sulfonate (TBA triflate, TBATf, Sigma-Aldrich, 99.99%), lithium bis(trifluoromethane sulfonyl)imide (LiTFSI, Gotion, 99.9%) were used as received. All chemicals were stored in an argon-filled MBRAUN glove box with oxygen content lower than 0.1 ppm, and water content

View Article Online
DOI: 10.1039/D0CP02568B

below 2 ppm. All solutions were prepared inside the glove box, and the water content, measured using a Karl Fischer coulometer titrator (831 KFCoulometer, Metrohm), was below 100 ppm in all cases, except when a different quantity is specified.

2.2 Electrochemical experiments

Electrochemical experiments were performed in a three-electrode cell under an Ar or O_2 atmosphere, with an Au working electrode and a Pt counter electrode. A Pt wire was painted with a $LiMn_2O_4/Li_2Mn_2O_4$ ink (80% equimolar mixture of the lithium manganese oxides, 10% Vulcan carbon and 10% polyvynilidene fluoride (PVDF) using n-methyl pyrrolidone as solvent) and placed in a fritted glass compartment. That compartment was filled with a 1M LiTFSI solution in DG and then used as reference electrode. Its open circuit potential vs a lithium wire (99.9% trace metals basis, Aldrich) submerged in the working solutions was measured inside the glovebox, and this potential was used to make the conversion to the Li^+/Li scale in the respective solvent. Even though 1.0 M electrolytes solutions are more commonly used in Li-O_2 batteries, in this work we use 0.1 M electrolyte solutions as it was recently proved that concentrations lower than 1.0 M do not significantly affect the cell stability.[20]

2.3 Infrared experiments

A Thermo Nicolet 8700 (Nicolet, Madison, WI) spectrometer equipped with a custom-made external table top optical mount and a MCTA detector was used for the electrochemical in situ subtractively normalized interfacial Fourier transform infrared spectroscopy (SNIFTIRS) experiments as described elsewhere.[15]

These experiments were carried out in a custom-made three-electrode Teflon electrochemical cell (see Figure S1) with a polycrystalline gold disc electrode aligned against CaF_2

View Article Online
DOI: 10.1039/D0CP02568B

window (a 25 mm CaF_2 equilateral prism, Harrick Scientific Technology). The cell was connected to a Jaissle IMP88 Potentiostat controlled by a computer via a digital-to-analog converter (Agilent USB AD/DA converter). The gold disc was set to be the working electrode, a Pt foil was used as counter electrode and all potentials were measured vs the same reference electrode described above. Typically, a few micrometers of electrolyte solution separated the electrode and the CaF2 window. In this configuration, the IR beam passes two times through the liquid layer. All the species formed or decomposed, adsorbed or that had migrated to the thin layer of electrolyte are detected by this technique and the sensibility is the same over the whole investigated spectral range.

For each system, a reference spectrum was taken at open circuit potential, R_0, and then the potential was varied in steps. Each step comprises an equilibration time of 120 s at a set potential, followed by the acquisition of an IR spectrum averaging 50 scans at 4 cm^{-1} resolution, R_E. The SNIFTIRS spectra is then calculated as $R=R_E/R_0$. Taking into account that R_0 is the reflectance of the reference spectrum, and R_E the reflectance of the sample spectrum, negative peaks, where $R_E<R_0$, are due to the formation of new species, and positive peaks, where $R_E>R_0$, correspond to the degradation of species.

Transmission spectra of the pure solvents were performed using a thin optical pass liquid cell with CaF_2 windows while spectra of the pure salts were performed using KBr pellets. The resolution was set to 4 cm^{-1} and 200 scans were performed.

Polarization modulation infrared reflection absorption spectroscopy (PM-IRRAS) experiments were performed on a Thermo Nicolet 8700 (Nicolet) spectrometer equipped with a custom-made external table-top optical mount, a MCT-A detector (Nicolet), a photoelastic modulator PEM (PM-90 with II/Zs50 ZnSe 50 kHz optical head, Hinds Instrument) and synchronous sampling demodulator SSD (GWC Instruments). The gold samples were mounted on an adjustable sample holder. The IR signal was maximized by adjusting the angle, height, and

View Article Online
DOI: 10.1039/D0CP02568B

position of the gold sample. The IR spectra were acquired with the PEM set for a half-wave retardation at 2900 cm^{-1} for the CH stretching and at 1500 cm^{-1} for the stretching modes associated with CF_3 and SO_2 groups.

The angle of incidence was set at 80º, which gives the maximum of mean square electric field strength for the air/gold interface. The demodulation technique developed by Corn[30] was used in this work. The signal was corrected by the PEM response using a method described by Frey *et. al*.[30]

3. RESULTS AND DISCUSSION

3.1 Stability of TEGDME under different operating conditions

In order to explore the intrinsic stability of the TEGDME solvent, we performed a series of experiments involving cyclic voltammetry and in situ IR spectroscopy at different Li-air battery operating conditions. We tested a typical Li-O_2 electrolyte, LiTFSI in TEGDME, either saturated with O_2 or Ar by cyclic voltammetry, as shown in Figure 1. In this work, the potential scale is always referred respect to the couple Li^+/Li, obtained as explained in the experimental section. The anionic sweep started at 3 V (OCP) in the positive direction until 4.4 V was reached. Afterwards, it was reversed into the negative direction down to 1.5 V and then returned to the initial potential. The same procedure was applied twice. During the cathodic scan a broad reduction peak centered around 2.1 V is observed, corresponding to a multiple-step process leading to lithium peroxide formation[31]. The first step of this process is the one-electron electrochemical reduction of O_2 to form a superoxide radical ($O_2^{-\bullet}$). In lithium-containing glyme-based electrolytes, the superoxide radical readily forms lithium superoxide on the electrode surface, which quickly disproportionates to form lithium peroxide.[1] On the anodic scan, the electrochemical oxidation of the previously

View Article Online
DOI: 10.1039/D0CP02568B

generated lithium peroxide can be observed.[32] The two electrochemical processes present at the potential domain between 3.0-3.7 V can be readily interpreted in terms of the lithium peroxide oxidation unified reaction mechanism recently proposed.[33] In low donicity solvents such as glymes, this two-steps surface mechanism involves a first electrochemical delithiation stage followed by an electrochemical oxidation of the delithiated products, leading to the complete decomposition of lithium peroxide into Li^+ and O_2.[33]

As it was expected, these two electrochemical processes are not observed in the Ar saturated electrolyte. It is interesting to note that a degradation current can be seen in the cyclic voltagramms at a potential > 3.6 – 3.9 V even during the first anodic scan (before lithium peroxide formation) and also in the experiments in absence of O_2 (Ar saturated electrolytes). This phenomenon has been reported previously for different long-chain glymes,[19,32] although the specific potential of occurrence is highly dependent on the nature and concentration of the salt used. A detailed analysis on its origin is still missing. Under O_2 atmosphere, that current is exacerbated, and appears as a third oxidation peak, centered at 3.9 V. In general, there is a quite good agreement that at this potential the main electrochemical process taking place is solvent decomposition.[21,32,34] The results shown in Figure 1 suggest that there is an intrinsic electro-chemical instability of the TEGDME solvent at potentials above 3.8 V, as TEGDME decomposition is observed even in the absence of any reactive oxygen species.

View Article Online
DOI: 10.1039/D0CP02568B

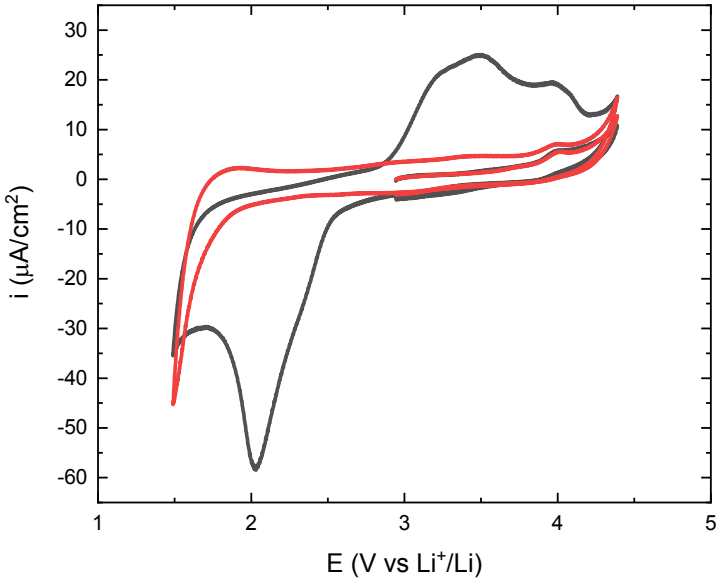

Figure 1: cyclic voltagramm of LiTFSI in TEGDME 0.1M at scan velocity: 0.1V/sec. Black curve: O_2 atmosphere, red curve: Ar atmosphere. Only the first cycle reduction peak is shown for more clarity.

With the purpose of bringing some light to the stability of the tetraglyme solvent in different operating conditions, SNIFTIRS experiments were performed on the aforementioned electrolyte in presence and absence of O_2. The step potentials were chosen between 1.5 V and 4.4 V based on the limits of stability seen in the cyclic voltammetry, and followed the same sequence.

A quick look at Figure 2 should draw the reader's attention to three main wavenumber ranges: from 2750 cm^{-1} to 3000 cm^{-1}, around 2300 cm^{-1} and from 1500 cm^{-1} to 1100 cm^{-1}. The region between 2750-3000 cm^{-1} corresponds to the stretching vibrations of CH_2 and CH_3 present in the glyme structure. The glymes have very high absorbance in this range, and the signal to noise ratio in SNIFTIRS experiments is very low. Since the presence of these bands in the spectra were not reproducible, they are not considered in our analysis.

View Article Online
DOI: 10.1039/D0CP02568B

The region between 1500 and 1100 cm^{-1} corresponds mostly to the anion absorption peak frequencies.[35] The peak at 1352 cm^{-1} can be assigned to SO_2 antisymmetric stretching ($\nu_{as}SO_2$) while the peak at 1186 cm^{-1} to CF_3 antisymmetric stretching ($\nu_{as}CF_3$) of $TFSI^-$.[36] A dependence of anion stretching peaks areas with potential can be noted. Figure 2.a) shows that these peaks are negative for E > 2.94 V and positive for E < 2.94 V. This trend is clearly observed during the first cycle of every experiment, becoming less marked as the electrode is further cycled. Figure S2 shows the dependence of the anion peaks area with time and potential, which is attributed to the electrostatic interaction between the anions and the working electrode. When the potential is higher than the open circuit voltage, anions are attracted to the surface of the working electrode, thus increasing their local concentration. This phenomenon results in a negative peak in SNIFTIRS spectra. The positive peaks at potentials < 2.94 V are attributed to the decrease in the local concentration of anions due to the low applied potentials. Thus, the spectra show the dependence of the population of the double layer on the working electrode. A similar behaviour has been reported before in acetonitrile.[37,38] After the first couple of cycles, the signals from the anions seem to be superimposed with other signals, probably due to a passivating film formed on the working electrode (see below). Hence, for some experiments, in the second or third cycle this trend is no longer observed, as it is the case for LiTFSI-TEGDME solution in Figure 2.b).

View Article Online
DOI: 10.1039/D0CP02568B

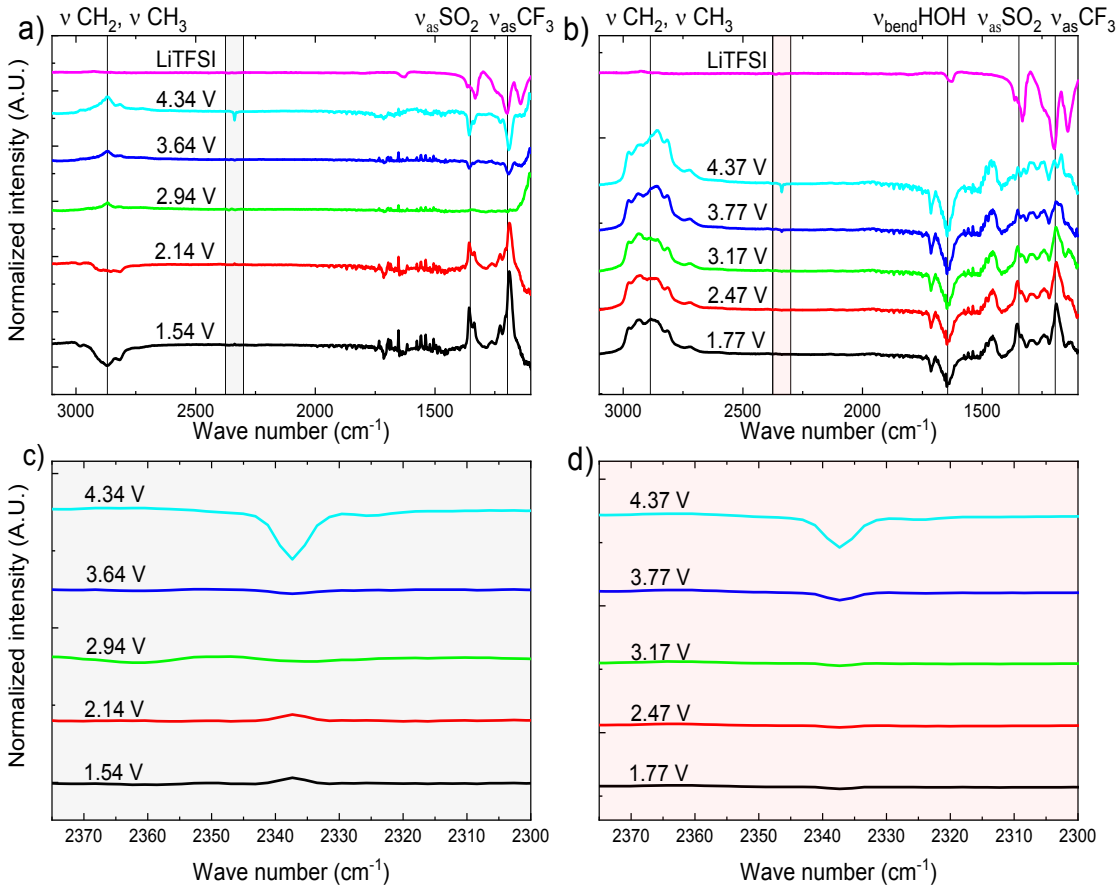

Figure 2: Upper panel: SNIFTIRS spectra of LiTFSI-TEGDME 0.1 M during the second anodic sweep a) in presence of O_2. b) in absence of O_2. Lower panel: Zoom in the coloured region of the previous panels for c) Solution saturated with O_2. d) Absence of O_2. Assignation of the most important peaks highlighted in the upper panel, for a detailed assignation please refer to the main text.

In the region around 2300 cm^{-1} the appearance of a negative peak at 2337 cm^{-1}, corresponds to the formation of surface adsorbed CO_2 at high potentials. The formation of CO_2 is due to the decomposition of the solvent[34,39,40] and appears both in the presence and absence of molecular oxygen, as shown in Figure 2. Signals corresponding to the formation of H_2O, an oxidative decomposition product as shown by Freunberger et al.[11] appear after the first cathodic sweep

View Article Online
DOI: 10.1039/D0CP02568B

around 3500 cm^{-1} (not shown) and 1650 cm^{-1} corresponding to the O-H stretching peak and the H-O-H scissoring peak of water respectively[41] in all the conditions tested for TEGDME.

Figure 3 shows the dependence of the CO_2 peak area as a function of applied potential. For potentials below 3.6 V, CO_2 evolution is practically negligible for both Ar and O_2 saturated electrolytes, while at potentials above 3.6 V, CO_2 appears in both cases, in greater quantities in the case of O_2 saturated electrolyte. This difference is amplified at the most extreme tested potential (4.6 V), where the quantity of CO_2 generated is roughly two times higher in the O_2 saturated electrolyte than in the Ar saturated solution. This fact clearly implies that oxygen promotes the decomposition of the solvent, but it is not the only cause as is evidenced by the amount of CO_2 produced in the oxygen free electrolyte. It has been widely proposed that the responsible species for glyme degradation are the oxygen reduction products formed due to the ORR during the discharge of the cell,[26,32,42] but in this case we detect CO_2 as a decomposition product *even* in absence of oxygen, therefore absence of reduced oxygen species (ROS). We consider that this oxidation of the tetraglyme correlates with the oxidation current observed in the CV in Figure 1. The difference in the onset voltage for CO_2 peak area rise in the IR experiments and the oxidation current on the voltammetry can be ascribed to the nature of the experiments: In the in situ spectroscopy experiment the electrode was polarized at different potentials, then the system was allowed to equilibrate at each step, while in the cyclic voltammetry the potential was scanned at a constant velocity, resulting in a linear dependence of the peak position with the scan rate.

CO_2 evolution in the Ar saturated solutions clearly exposed the intrinsic electrochemical stability problems of the TEGDME-based electrolytes.

View Article Online
DOI: 10.1039/D0CP02568B

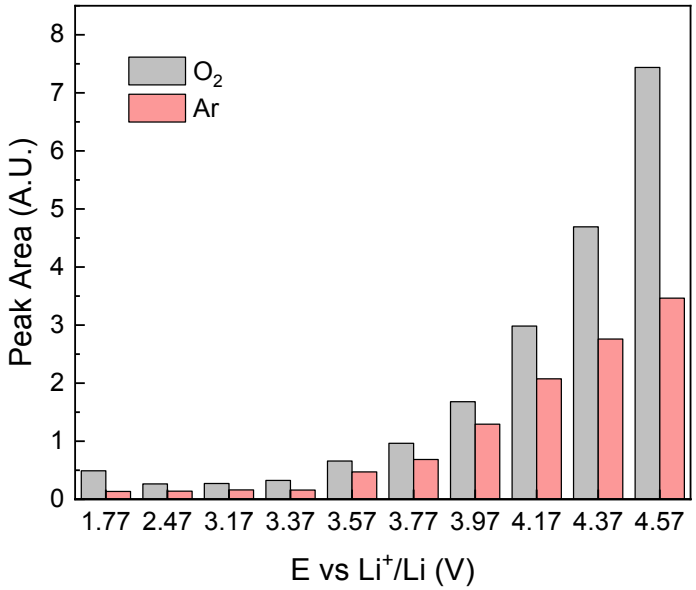

Figure 3: Absolute value of the CO_2 peak area for 0.1M solutions of LiTFSI-TEGDME as a function of potential in presence or absence of O_2.

We also explored the effect of the chemical nature of the salt used in the process of solvent decomposition. Figure 4.a) shows the CV of TEGDME with three different salts in Ar atmosphere. It is interesting to note that for LiTf, TBATf, and LiTFSI a small oxidation current is always present at 3.7 - 3.9 V. When comparing the carbon dioxide peak areas at different potentials (Figure 4.b), it is evident that the use of LiTf as electrolyte salt leads to a more stable system than when LiTFSI is used. The aforementioned peak appears at higher potentials and is smaller for LiTf salt up to 4.2V, although there is always some decomposition. Given the lower ionic association strength of LiTFSI compared to LiTf in these glymes,[43] the amount of free Li^+ able to strongly interact with TEGDME is higher, which results in the polarization and consequent destabilization of the solvent molecules. In the case of TBATf, the CO_2 is formed at ~3V, and its concentration on the electrode remains almost constant. Furthermore, this process does not seem to correlate with the rise of the

View Article Online
DOI: 10.1039/D0CP02568B

oxidation current potential in the CV (at 3.65 V). This behaviour might be ascribed to the chemical decomposition of the glyme in the presence of TBA^+ cation decomposition products.[44]

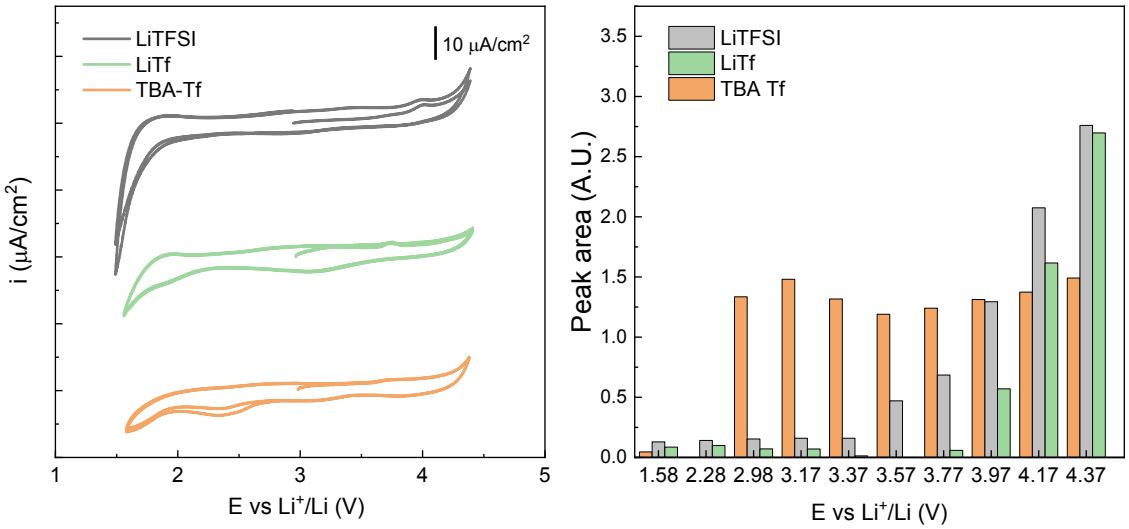

Figure 4: a) Cyclic voltammetry of three different salts at 0.1M concentration in TEGDME solution under Ar atmosphere, displaced in the Y axes for more visual clarity. b) Absolute value of the area of the CO_2 peak as a function of potential in the absence of O_2.

In order to analyze the decomposition products remaining on the electrode surface, Figure S3 shows the PM-IRRAS spectrum of the electrode surface after 2 hs polarization at 4,4 V in a 0.1M LiTFSI-TEGDME solution. The electrode was rinsed with water, ethanol and dried with N_2 before taking the spectrum, which shows broad peaks at around 2800 cm^{-1} that can be assigned to CH_2 and CH_3 stretching. Furthermore, the peaks between 1500 cm^{-1} and 1100 cm^{-1} can be attributed to TEGDME, as it can be seen from comparison with the transmission spectrum of the solvent, also shown in Figure S3. It is possible that TEGDME forms potential-induced polymers, usually known as solid electrolyte interphase, which forms a film in the surface that stays even after rinsing. There is no significant evidence of the presence of the lithium salt in that film from the spectra shown.

View Article Online
DOI: 10.1039/D0CP02568B

Even when the most accepted theory is that either reduced oxygen species or singlet oxygen are the responsible ones for solvent degradation, we have shown that TEGDME is intrinsically unstable: degradation occurs between 3.6 - 3.9 V vs Li^+/Li even in the absence of oxygen and lithium. This decomposition potential is extremely close to the OER potential, making the deconvolution of the two processes a highly complex task. The overall conclusion is that a TEGDME-based lithium-air battery will not be successful without the addition of a redox-mediator to lower the charging overpotentials, and so, avoiding solvent decomposition.

3.2 Stability of diglyme and the effect of water content

Cyclic voltammetry using a polished Au electrode in a 0.1M LiTFSI solution in DG saturated either in O_2 or Ar are displayed in Figure 5. In the presence of oxygen, an oxidation peak corresponding to solvent degradation occurs at 4.25 V, and there is no oxidation current under Ar atmosphere. This is a clear evidence of the higher stability of the DG-based electrolyte over the TEGDME-based electrolytes, as previously shown comparing the electrochemical performance of DG and TEGDME-based electrolytes by means of galvanostatic charge/discharge experiments with batteries under prolonged cycling.[20]

View Article Online
DOI: 10.1039/D0CP02568B

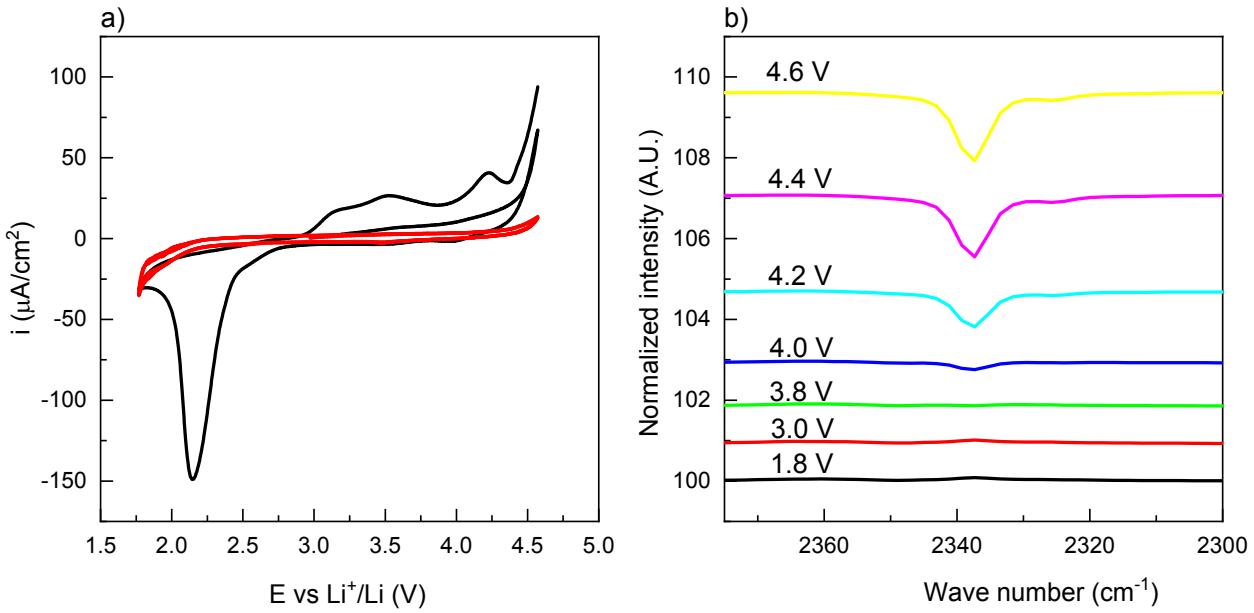

Figure 5: a) Cyclic voltammetry of a 0.1M solution of LiTFSI in DG under O_2 (black curve) and Ar (red curve) atmosphere. Scan velocity: 0.1V/sec. b) SNIFTIRS spectra of LiTFSI-DG 0.1 M in presence of O_2 in the region 2375 – 2300 cm^{-1} where the adsorbed CO_2 signal is present.

Following the same procedure described before, SNIFTIRS experiments were done with the DG-based electrolyte. The step potentials were chosen between 1.8 V and 4.6 V based on the limits of solvent stability shown in the cyclic voltammetry. Figure S4 shows some of the in situ IR spectra taken at different potentials. Once again, a dependence of the anion peaks (1500 - 1100 cm^{-1} region) with potential can be seen: for high potentials, negative peaks appear indicating that the anion concentrates in the vicinity of the electrode, and for low potentials the appearance of positive peaks can be seen, indicating their "local dilution". A negative adsorbed CO_2 peak also appears at high potential, indicating the instability of the solvent at potentials above 4.0 V, as shown in detail in Figure 5b).

Since DG showed a higher stability in the Li-O_2 battery work conditions, further experiments were carried out, to study how the concentration of water present in the system affects

View Article Online
DOI: 10.1039/D0CP02568B

its stability. This is an especially important topic because in the scientific community there is a big deal of controversy on the use of water as a suitable electrolyte's additive.[1,25–29]

Figure 6 depicts the integrated area of CO_2 peak for LiTFSI- DG solutions with different amounts of water, along with the corresponding applied potential. A quick examination of Figure 6.a) denotes the similarity of the electrolyte containing low and high amounts of water (90 and 2500 ppm respectively) in terms of the amount of CO_2 produced as a result of applied potential. Interestingly, carbon dioxide is formed even in the first anodic sweep, where there is no O_2^{2-} or Li_2O_2 present. At low potentials, the signal disappears due to the diffusion of the CO_2 into the solution, which is discussed in more detail later on. Data shown in Figure 6.b), which highlights the second anodic sweep portrayed in Figure 6.a), shows a rise in CO_2 peak area at potentials higher than 4.0 V for the electrolyte with low water content and E > 3.4 V for the one with high water content. It also confirms that the addition of 2500 ppm of water does not significantly affect the area of the adsorbed CO_2 peak at potentials > 4.2 V, even though it seems that the decomposition starts at lower potentials when water is present.

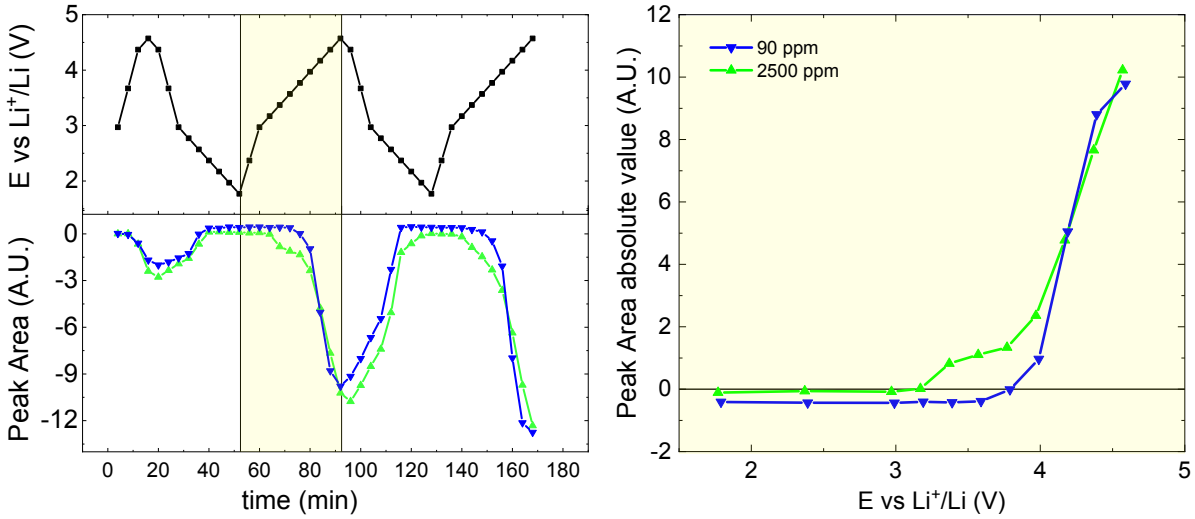

Figure 6: a) Area of adsorbed CO_2 peak compared to potential applied for a 0.1M solution of LiTFSI in DG with different water concentrations. b) Absolute value of the same peak area vs potential for the second anodic sweep, highlighted with yellow in the first panel. Blue line corresponds to 90 ppm, green line corresponds to 2500 ppm.

View Article Online
DOI: 10.1039/D0CP02568B

To further study the process that takes place at 4.25 V seen in Figure 6, the electrode was cycled between 1.8 V and 4.6 V, and then the potential was held constant at 4.25 V for 4.5 hours. Also, for one of the solutions containing approximately 2500 ppm of water, the potential was then maintained at 0 V for another 4.5 hs. IR spectra were taken at each step potential, and the CO_2 area was integrated. The results are depicted in Figure 7.

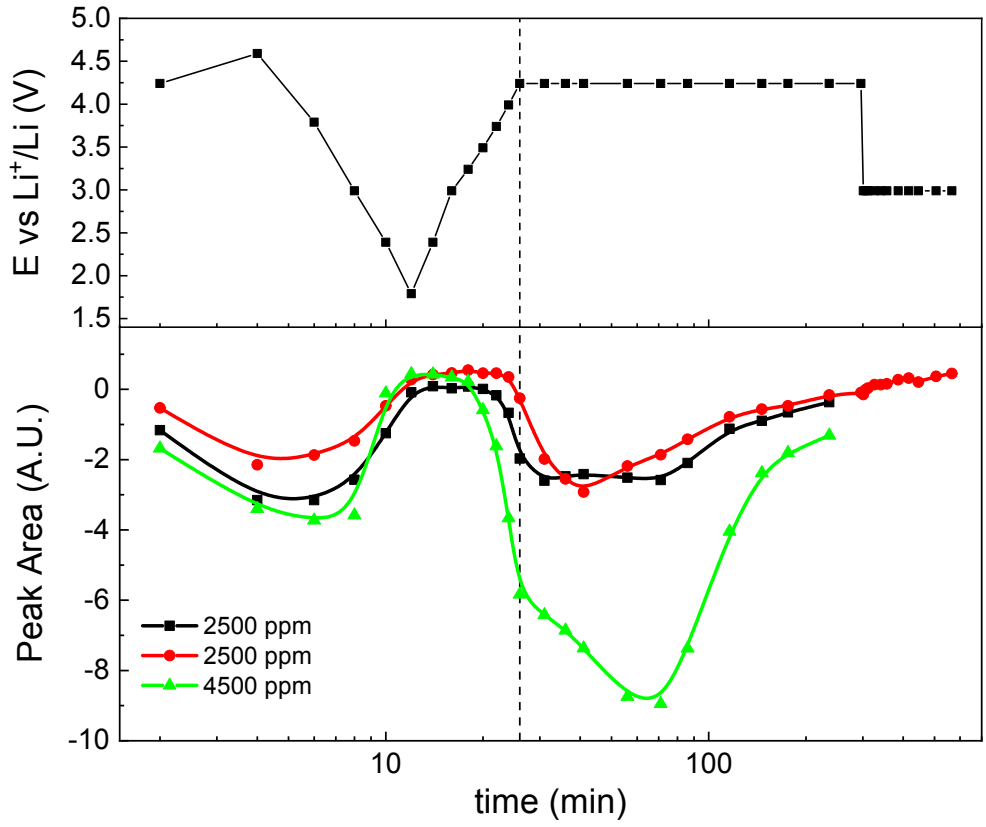

Figure 7: Area of adsorbed CO_2 peak at different applied potentials for a 0.1M LiTFSI solution in DG with different contents of water. Red and black lines: 2500 ppm of water (duplicates), green line: 4500 ppm of water. Time axes is showed in logarithmic scale.

In Figure 7, it can be observed that the CO_2 peak area starts growing at potential < 4.25V (marked with a dashed line) and continues to grow when the potential is held constant. Eventually, a decrease in the signal is observed, which can be explained by the formation of a passivation film

View Article Online
DOI: 10.1039/D0CP02568B

in the surface of the electrode composed of DG decomposition products (shown in Figure S5). When the electrode is passivated, the decomposition rate, and thus the generation rate of CO_2 decreases and its diffusion to the bulk solution becomes the predominant process. More interestingly, Figure 7 also shows that the addition of 4500 ppm of water does affect the degradation rate of the diglyme. This effect is only noted after the first cathodic sweep, that is, when reduced oxygen species are present, which is indicative of water taking part in the ROS-originated decomposition.

Although some mechanisms for polyether decomposition in Li-air battery under certain conditions have been proposed,[11,32] none of them involve water as a reactive. Their inability to predict the correlation between degradation rate and water concentration brings to light the lack of a complete understanding of these intricate chemical systems. In light of recent work,[25,26,45] a plausible explanation for this correlation is that the presence of water promotes the formation of singlet oxygen species during the cathodic and anodic sweeps. It is known that the superoxide anion disproportionation leads to the formation of singlet oxygen in organic solvents with low water content when the amount of water is enough to hexacoordinate the dissolved O_2^{-}.[25,26,46–48] When this condition is met, disproportionation results in hydrogen peroxide and singlet oxygen which triggers chemical solvent degradation. The resulting electrochemically unstable species would then further oxidize during the anodic sweep, leading to an acceleration of CO_2 evolution. Further studies regarding the dependence of singlet oxygen formation with water concentration are essential to shed some light into these complex processes.

4. CONCLUSIONS

View Article Online
DOI: 10.1039/D0CP02568B

We have studied the stability of two glymes as solvents in Li^+ electrolyte for the Li–air battery. In situ SNIFTIRS experiments showed that TEGDME is intrinsically unstable and degradation occurs between 3.6 - 3.9 V vs Li^+/Li even in the absence of oxygen and lithium. This decomposition potential is extremely close to the OER potential, so TEGDME-based lithium-air battery will not be successful without the addition of a redox-mediator to lower charging overpotentials and avoid solvent decomposition. On the other hand, DG showed a higher stability, with a degradation onset potential higher than 4,0 V under operating conditions (presence of lithium and saturated in oxygen). Great care must be taken regarding the presence of water, since it has a direct influence both on the rate of solvent decomposition and the onset potential where it occurs, probably related to singlet oxygen generation.

CONFLICTS OF INTEREST

There are no conflicts to declare.

ACKNOWLEDGMENTS

LMDL, EdL and EJC are research staff of CONICET. GH acknowledges CONICET for her doctoral fellowship**.** EdL thank financial support from Agencia Nacional de Promoción Científica y Tecnológica (ANPCyT) (PICT 2017-2414).

REFERENCES

1 W.-J. Kwak, Rosy, D. Sharon, C. Xia, H. Kim, L. R. Johnson, P. G. Bruce, L. F. Nazar,

View Article Online
DOI: 10.1039/D0CP02568B

Y.-K. Sun, A. A. Frimer, M. Noked, S. A. Freunberger and D. Aurbach, *Chem. Rev.*, , DOI:10.1021/acs.chemrev.9b00609.

2 P. G. Bruce, S. A. Freunberger, L. J. Hardwick and J.-M. Tarascon, *Nat. Mater.*, 2012, **11**, 19–29.

3 N. Imanishi, A. C. Luntz and P. Bruce, Springer New York, New York, NY, 2014.

4 J. Lu, L. Li, J.-B. Park, Y.-K. Sun, F. Wu and K. Amine, *Chem. Rev.*, 2014, **114**, 5611–5640.

5 L. Ma, T. Yu, E. Tzoganakis, K. Amine, T. Wu, Z. Chen and J. Lu, *Adv. Energy Mater.*, 2018, **8**, 1800348.

6 X. Zhang, A. Chen, M. Jiao, Z. Xie and Z. Zhou, *Batter. Supercaps*, 2019, **2**, 498–508.

7 B. D. McCloskey, C. M. Burke, J. E. Nichols and S. E. Renfrew, *Chem. Commun.*, 2015, **51**, 12701–12715.

8 B. D. McCloskey, D. S. Bethune, R. M. Shelby, G. Girishkumar and A. C. Luntz, *J. Phys. Chem. Lett.*, 2011, **2**, 1161–1166.

9 W. Xu, K. Xu, V. V Viswanathan, S. A. Towne, J. S. Hardy, J. Xiao, Z. Nie, D. Hu, D. Wang and J.-G. Zhang, *J. Power Sources*, 2011, **196**, 9631–9639.

10 S. A. Freunberger, Y. Chen, Z. Peng, J. M. Griffin, L. J. Hardwick, F. Bardé, P. Novák and P. G. Bruce, *J. Am. Chem. Soc.*, 2011, **133**, 8040–8047.

11 S. A. Freunberger, Y. Chen, N. E. Drewett, L. J. Hardwick, F. Bardé and P. G. Bruce, *Angew. Chemie Int. Ed.*, 2011, **50**, 8609–8613.

12 Y. Chen, S. A. Freunberger, Z. Peng, F. Bardé and P. G. Bruce, *J. Am. Chem. Soc.*, 2012, **134**, 7952–7957.

13 F. Bardé, Y. Chen, L. Johnson, S. Schaltin, J. Fransaer and P. G. Bruce, *J. Phys. Chem. C*, 2014, **118**, 18892–18898.

View Article Online
DOI: 10.1039/D0CP02568B

14 B. D. McCloskey, D. S. Bethune, R. M. Shelby, T. Mori, R. Scheffler, A. Speidel, M. Sherwood and A. C. Luntz, *J. Phys. Chem. Lett.*, 2012, **3**, 3043–3047.

15 N. Mozhzhukhina, L. P. Méndez De Leo and E. J. Calvo, *J. Phys. Chem. C*, 2013, **117**, 18375–18380.

16 D. G. Kwabi, T. P. Batcho, C. V. Amanchukwu, N. Ortiz-Vitoriano, P. Hammond, C. V. Thompson and Y. Shao-Horn, *J. Phys. Chem. Lett.*, 2014, **5**, 2850–2856.

17 D. Xu, Z. Wang, J. Xu, L. Zhang and X. Zhang, *Chem. Commun.*, 2012, **48**, 6948.

18 C. O. Laoire, S. Mukerjee, E. J. Plichta, M. A. Hendrickson and K. M. Abraham, *J. Electrochem. Soc.*, 2011, **158**, A302.

19 H. G. Jung, J. Hassoun, J. B. Park, Y. K. Sun and B. Scrosati, *Nat. Chem.*, 2012, **4**, 579–585.

20 D. Sharon, D. Hirshberg, M. Afri, A. A. Frimer and D. Aurbach, *Chem. Commun.*, 2017, **53**, 3269–3272.

21 A. Chamaani, M. Safa, N. Chawla, M. Herndon and B. El-Zahab, *J. Electroanal. Chem.*, 2018, **815**, 143–150.

22 K. U. Schwenke, S. Meini, X. Wu, H. A. Gasteiger and M. Piana, *Phys. Chem. Chem. Phys.*, 2013, **15**, 11830–11839.

23 B. D. Mccloskey, A. Valery, A. C. Luntz, S. R. Gowda, G. M. Wallraff, J. M. Garcia, T. Mori and L. E. Krupp, *J. Phys. Chem. Lett.*, 2013, **4**, 2989–2993.

24 M. Carboni, A. G. Marrani, R. Spezia and S. Brutti, *J. Electrochem. Soc.*, 2018, **165**, A118–A125.

25 J. Wandt, P. Jakes, J. Granwehr, H. A. Gasteiger and R. A. Eichel, *Angew. Chemie - Int. Ed.*, 2016, **55**, 6892–6895.

26 N. Mahne, B. Schafzahl, C. Leypold, M. Leypold, S. Grumm, A. Leitgeb, G. A.

View Article Online
DOI: 10.1039/D0CP02568B

Strohmeier, M. Wilkening, O. Fontaine, D. Kramer, C. Slugovc, S. M. Borisov and S. A. Freunberger, *Nat. Energy*, 2017, **2**, 1–9.

27 T. Liu, M. Leskes, W. Yu, A. J. Moore, L. Zhou, P. M. Bayley, G. Kim and C. P. Grey, *Science*, 2015, **350**, 530–533.

28 W.-J. Kwak, D. Hirshberg, D. Sharon, H.-J. Shin, M. Afri, J.-B. Park, A. Garsuch, F. F. Chesneau, A. A. Frimer, D. Aurbach and Y.-K. Sun, *J. Mater. Chem. A*, 2015, **3**, 8855–8864.

29 C. M. Burke, R. Black, I. R. Kochetkov, V. Giordani, D. Addison, L. F. Nazar and B. D. McCloskey, *ACS Energy Lett.*, 2016, **1**, 747–756.

30 B. L. Frey, R. M. Corn and S. C. Weibel, in *Handbook of Vibrational Spectroscopy*, ed. P. R. Griffiths, John Wiley & Sons, Ltd, Chichester, UK, 2006.

31 D. Sharon, D. Hirsberg, M. Salama, M. Afri, A. A. Frimer, M. Noked, W. Kwak, Y. K. Sun and D. Aurbach, *ACS Appl. Mater. Interfaces*, 2016, **8**, 5300–5307.

32 D. Sharon, V. Etacheri, A. Garsuch, M. Afri, A. A. Frimer and D. Aurbach, *J. Phys. Chem. Lett.*, 2013, **4**, 127–131.

33 Y. Wang, N. C. Lai, Y. R. Lu, Y. Zhou, C. L. Dong and Y. C. Lu, *Joule*, 2018, **2**, 2364–2380.

34 S. Meini, S. Solchenbach, M. Piana and H. A. Gasteiger, *J. Electrochem. Soc.*, 2014, **161**, A1306–A1314.

35 N. Mozhzhukhina, A. Y. Tesio, L. P. Mendez De Leo and E. J. Calvo, *J. Electrochem. Soc.*, 2017, **164**, A518–A523.

36 I. Rey, P. Johansson, J. Lindgren, J. C. Lassègues, J. Grondin and L. Servant, *J. Phys. Chem. A*, 1998, **102**, 3249–3258.

37 S. Pons and T. Davidson, *J. Electroanal. Chem.*, 1982, **140**, 211–216.

View Article Online
DOI: 10.1039/D0CP02568B

38 T. Davidson, B. S. Pons, A. Bewick and P. Schmidt, *J. Electroanal. Chem.*, 1981, **125**, 237.

39 N. Tsiouvaras, S. Meini, I. Buchberger and H. A. Gasteiger, *J. Electrochem. Soc.*, 2013, **160**, A471–A477.

40 M. Balaish, A. Kraytsberg and Y. Ein-Eli, *Phys. Chem. Chem. Phys.*, 2014, **16**, 2801–2822.

41 D. Lin-Vein, N. B. Colthup, W. B. Fateley and J. G. Grasselli, Academic Press Inc, San Diego, CA, 1941.

42 A. C. Luntz and B. D. McCloskey, *Nat. Energy*, 2017, **2**, 17056.

43 G. Horwitz, M. Factorovich, J. Rodriguez, D. Laria and H. R. Corti, *ACS Omega*, 2018, **3**, 11205–11215.

44 C. V. Amanchukwu, H. H. Chang and P. T. Hammond, *J. Phys. Chem. C*, 2017, **121**, 17671–17681.

45 E. Mourad, Y. K. Petit, R. Spezia, A. Samojlov, F. F. Summa, C. Prehal, C. Leypold, N. Mahne, C. Slugovc, O. Fontaine, S. Brutti and S. A. Freunberger, *Energy Environ. Sci.*, 2019, **12**, 2559–2568.

46 A. U. Khan, *Photochem. Photobiol.*, 1978, **28**, 615–626.

47 D. Córdoba, H. B. Rodríguez and E. J. Calvo, *Chem. Sel.*, 2019, **4**, 12304–12307.

48 I. Lozano, D. Córdoba, H. B. Rodríguez, I. Landa-Medrano, N. Ortiz-Vitorino, T. Rojo, I. Ruiz de Larramendia and E. J. Calvo, *J. Electroanal. Chem.*, 2020, in press.

View Article Online
DOI: 10.1039/D0CP02568B

TABLE OF CONTENTS ARTWORK

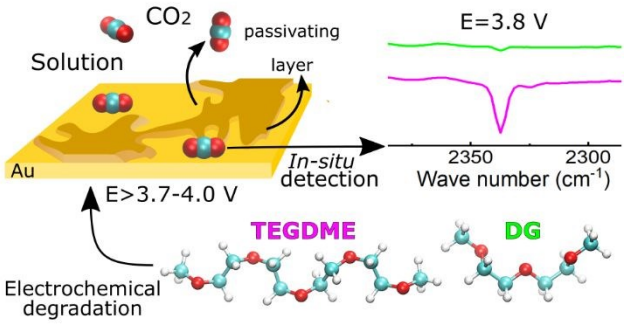

Tetraglyme-based electrolytes are intrinsically unstable even in the absence of oxygen and lithium ions, while diglyme-based electrolytes show better stability the addition of water exacerbates its decomposition.